

Back-analysis of settlement calculation for a raft foundation on CMC© using the appropriate strain range

Brûlé Stéphane, Pablo Gervu Teixeira Dos Santos
 Menard, Orsay, France, stephane.brule@menard-mail.com

ABSTRACT: The settlement calculation of raft foundations for residential projects with basements requires an appropriate description of both unloading and loading moduli. It is also essential to consider deformation moduli estimated within the relevant strain range. In this article, we examine the real case of a project founded on soil reinforced with CMC© rigid inclusions. We compare theoretical and observed settlements with the objective of identifying the most appropriate deformation modulus. The example presented in the article provides an opportunity to test, through settlement measurements, the method for estimating deformation moduli, drawing in particular on the results of the French national research project ARSCOP.

KEYWORDS: Raft, rigid inclusions, CMC, settlement, back-analysis, strain range.

1 INTRODUCTION

The advancement of city modernization, particularly the development of buildings in urban areas, has led to the frequent presence of multi-story buildings with more than one basement level, which often poses a challenge during the design phase of new projects in major urban centers. In this urban context, one of the foundation solutions adopted is the use of shallow foundation systems with raft slabs, combined with ground improvement techniques using rigid inclusions such as Controlled Modulus Columns (CMC©), to treat more than 10 meters of fine soil with low mechanical properties. One of the main challenges identified is the difficulty in accurately estimating the deformation modulus within the appropriate strain range, which will be analyzed through a comparison between theoretical settlements and measured settlements on similar projects.

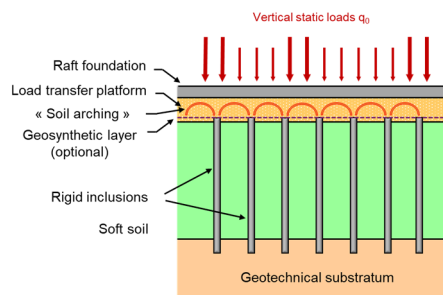


Figure 1. Principle of a raft-type foundation on rigid inclusions anchored on the geotechnical substratum. The load transfer platform (LTP) improves load transfer to the heads of rigid inclusions through a soil arching effect.

In this article, we first recall the principle of soil reinforcement using rigid inclusions beneath a raft and then address the issue of unloading and reloading modulus E . We describe the design principle based on vertical stiffness. We also discuss the French ARSCOP project, which aims to better characterize deformation moduli E according to the strain range corresponding to the applied load. The final part of the article presents a real case designed using ARSCOP data, for which settlement monitoring is available.

2 RAFT FOUNDATION ON RIGID INCLUSIONS

2.1 Principle

For this article, we discuss the case of building rafts with one or more basement levels, where the installation of rigid inclusions is carried out from the excavation bottom, on a working platform that will form part of the load transfer

platform (Figure 1). We are in a configuration where the soil has been unloaded by several meters of thickness (Figure 2). The weight of the excavated soil can even exceed that of the building project. With two basement levels reaching a depth of 6 m, the load balance may result in a net load applied to the ground close to zero. For a raft foundation, the primary design considerations include absolute settlement and, more critically, the spatial distribution of differential settlements. The latter has a substantial influence on structural reinforcement design.

2.2 Discussion on the vertical stress path σ_z

The phasing of the works involves a variation in the vertical stress σ_z for the soils located beneath the raft. Figure 2 illustrates this phasing.

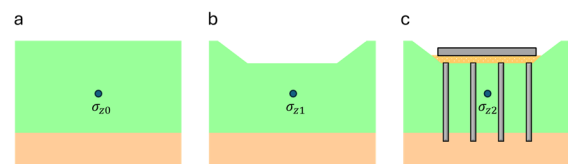


Figure 2. Main phasing steps. Initial conditions (a), excavation works (b), CMCs, LTP and the raft construction (c). Considering a reference point located beneath the raft (blue disk), we observe the variation of the vertical stress at this point, which changes from σ_{z0} to σ_{z2} .

From a rigorous perspective, the foundation subgrade may be subjected to substantial unloading followed, in certain cases, by significant reloading, potentially exceeding the initial stress state σ_{z0} (Figure 3). At a given depth z beneath the raft, the final stress will be $\sigma_{z0} + \Delta\sigma_z$. In Geotechnics, an issue frequently addressed during the design phase concerns the applicability of an unloading modulus for accurately estimating the anticipated deformation moduli.

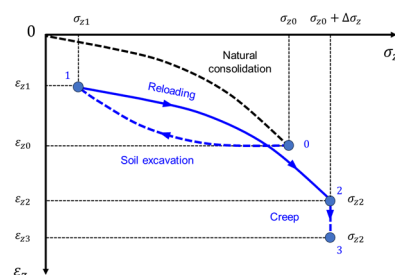


Figure 3. Vertical stress path (σ_z, ϵ_z) for a sequence involving excavation followed by loading from the structure. ϵ_z is the vertical strain of the soil. Point 0 corresponds to the initial state, point 1 to the stress level after unloading, point 2 to the stress induced by the weight of the structure, and Point 3 to the onset of creep over the service life of the structure.

In most projects, determining the value of the reloading modulus proves challenging, and it is frequently approximated as being equivalent to the initial loading modulus. How can the impact of this parameter selection approximation be assessed?

2.3 Discussion on the moduli for settlement calculation

Let us examine the different moduli based on the principle of a uniaxial compression test on a cylindrical sample (Figure 4).

Finite element analysis tools frequently require the E_{50} modulus, defined as the secant modulus corresponding to 50% of the failure stress.

The use of a secant modulus E_{sec} provides a means to analyze the evolution of the stress–strain relationship, particularly during the onset of plastic deformation. This modulus can be evaluated at very small strain levels, where the determination of the tangent modulus E_{tan} becomes increasingly challenging due to the high resolution required. As an alternative to the initial E_{ini} or secant modulus, a cyclic modulus E_{cyclic} may be derived from low amplitude unloading cycles. The modulus obtained through this approach is frequently higher than the initial modulus ($E_{cyclic} > E_{ini}$). According to Reiffsteck et al. (2018), the most reliable method for determining elastic moduli is through unloading tests.

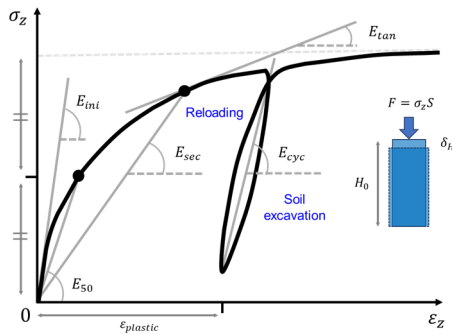


Figure 4. Definition of the different moduli (inspired by Reiffsteck et al., 2018) from a uniaxial compression test on a cylindrical sample (S is the surface of the sample, F , the vertical load applied, H_0 , the initial height of the cylinder, δ_H , vertical shortening of the cylinder).

Typically, the Ménard modulus E_M , obtained from the eponymous pressuremeter test (Ménard, 1955), provides a secant modulus calculated over a strain range that already extends into the plastic domain ($E_{ini} > E_M$). For settlement calculations, this modulus therefore almost always requires correction.

If the cyclic modulus (assimilated to reloading modulus) is closer to the real elastic modulus, and if the initial modulus is lower than the cyclic modulus, then adopting E_{ini} for calculations after soil excavation, makes the approach conservative with respect to settlements, as it will tend to overestimate them.

However, if the data obtained from investigations is a pressuremeter modulus E_M , it is necessary to derive a reliable estimate of the initial modulus E_{ini} . To this end, we examine the findings of the ARSCOP project (see §3).

2.4 Subgrade reaction modulus

The vertical deformation characteristics of the foundation are defined by independent, closely spaced, discrete and linearly elastic springs. This relatively simple mechanical representation of the soil foundation was first introduced by Winkler (1867). The proportionality constant of these springs is known as the subgrade reaction modulus, $k_s = \sigma_0/u_z$ (N/m^3 or MPa/m), with σ_0 the vertical applied stress (Figure 1) on the raft and u_z , the settlement. In this case, we obtain a map of k_s

values at the project scale (Figure 5), before and after reinforcement with rigid inclusions (Figure 6), which will most often reduce settlement by a factor of 3 to 7. This highlights the importance of a realistic characterization of the modulus E for settlement calculations.

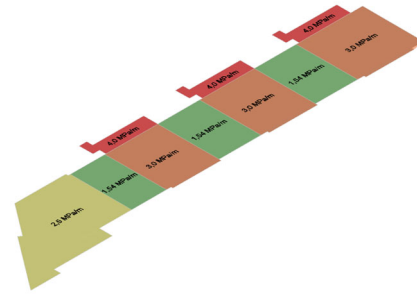


Figure 5. Subgrade stiffness map for the raft foundation project. Here, the k_s values range between 1.5 and 4.0 MPa/m .

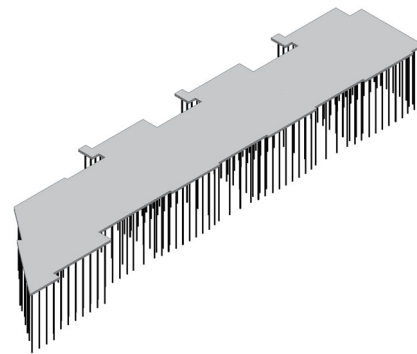


Figure 6. 3D model of soil reinforcement by rigid inclusion CMC under the raft.

3 IMPACT OF THE ARSCOP PROJECT ON THE DESIGN OF RAFT FOUNDATIONS

3.1 ARSCOP

Since the creation of the pressuremeter (Ménard, 1957; Baguelin et al., 1973; Gambin et Frank, 1982; Gambin, 1990. Briaud, 2013), both the equipment and the testing protocol have evolved (Arsonnet et al., 2005; Burlon et al., 2016), and the drilling and testing methodology has been standardized since 1990 through successive versions of the NF P94-110 standard, ultimately leading to the European standard NF EN ISO 22476-4 (AFNOR, 2015, 2021).

The French national research project ARSCOP (Les Nouvelles Approches de Reconnaissance des Sols et de Conception des Ouvrages géotechniques avec le Pressiomètre - New Approaches to Soil Investigation and Geotechnical Design Using the Pressuremeter), conducted from 2016 to 2024 (ARSCOP, 2024), aimed primarily at preserving the distinctive features of the pressuremeter test—namely, the pressure–volume curve obtained from a small-scale loading test, the stress state, the deformation modulus (E_M), and the strength parameter (p_{IM}^*) while continuing to refine and enhance the testing protocol.

The project was administered by IREX (Institut pour la Recherche appliquée et l'EXpérimentation en génie civil - Institute for Applied Research and Experimentation in Civil Engineering). One of the main results of ARSCOP is to specify the value of the soil deformation modulus $E = kE_M$ as a function of soil type and the range of strain ϵ under the applied load at the Earth's surface (Figure 7).

In the context of settlement analysis under large-scale loading, Combarieu highlighted, because the method was

initially defined for shallow foundations, that « a formulation of the type $E = \kappa E_M/\alpha$ offers a more suitable framework, with κ being a function of soil type, structural dimensions, and strain level—particularly at very low strains. This approach diminishes the relevance of the Ménard rheological factor α » (Combarieu, 2006).

The other topics addressed are advanced drilling and self-drilling techniques, specialized equipment and testing protocols to accurately capture soil behaviour in the small-strain range.

In addition, cyclic pressuremeter systems have been engineered to facilitate the investigation of soil liquefaction phenomena. Seismic pressuremeter devices have also been optimized to improve signal quality and enhance measurement efficiency (ARSCOP, 2024).

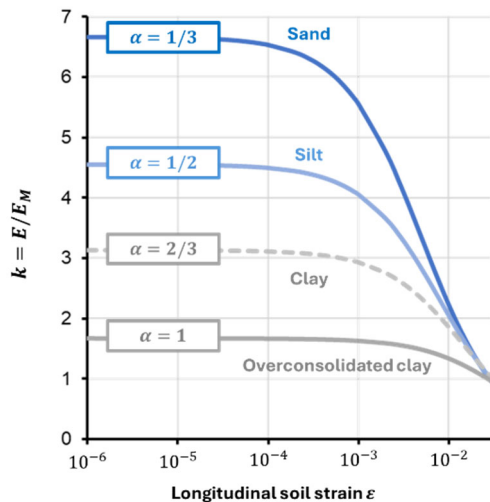


Figure 7. «k-curves», inspired from ARSCOP (ARSCOP, 2023). α is the Ménard rheological factor, E is the modulus for the strain range of interest and E_M is the Ménard modulus (Brûlé, 2025).

4 CASE STUDY

4.1 Main characteristics of the studied site

The case study concerns a site located in the municipality of Moirans, in the Isère department (France). Formerly occupied by industrial facilities, it has been redeveloped into a residential complex comprising 300 housing units and 900 m² of retail space, distributed across 19 buildings of up to four stories. The raft foundation was constructed at an elevation approximately matching the original natural ground level. Here, we focus on the raft foundation that required the deepest reinforcement with rigid inclusions. The serviceability limit state (SLS) uniform loads range between 40 and 120 kPa. According to standards EN 1998 (Eurocode 8), the structure is located in french seismic zone 4 and the importance factor for the building class II should be 1.0.

The aim of the rigid inclusion soil improvement was to achieve an absolute settlement not exceeding 3 cm. The allowable differential settlements are set at 1/500. We applied the principle of the anticipated results from the ARSCOP project (Hoang et al., 2018; Hoang et al., 2020).

The rigid inclusion works were carried out in september 2019, and settlements were monitored using a topographic target-survey method over a period of 400 days during the progressive construction of the building floors.

4.2 Geotechnical model

The geotechnical model is composed of seven layers, as detailed in Table 1. The overall thickness is 26 m. The groundwater table was located between 1 m and 2.6 m below

the natural ground surface. The initial model was refined through additional cone penetration tests (CPT).

Table 1. Geotechnical layer description. E_M is the pressuremeter modulus, α , the Ménard rheological factor, q_c , cone tip resistance.

Soil layer	Thickness	E_M	α	q_c	
Unit	(m)	MPa	-	MPa	
1	LTP	0.5	20	1/4	10
2	Clayey silt	5.7	1.8	1/2	0.6
3	Gravelly sand	3.4	11.3	1/3	8.5
4	Very soft silt	6.2	2.5	1/2	0.9
5	Soft silt	2.1	4.0	1/2	1.1
6	Medium silt	8.5	5.5	1/2	1.5
7	Gravelly sand	10.0	1/3	3.0	

We used the ARSCOP relationship $E = \kappa E_M$ to determine a design modulus for each layer, according to its lithology. To account for geological uncertainty, we applied a safety factor of 1.5 to obtain the design E_d values.

Table 2. Geotechnical layer description. $E = \kappa E_M$. The design values are E_d

Soil layer	Thickness	E	E_d
Unit	(m)	MPa	-
1	LTP	0.5	50
2	Clayey silt	5.7	7.2
3	Gravelly sand	3.4	62
4	Very soft silt	6.2	10
5	Soft silt	2.1	16
6	Medium silt	8.5	22
7	Gravelly sand	55	36.7

4.3 Ground reinforcement program

The Controlled Modulus Columns (CMC©) with a diameter of 320 mm are embedded 50 cm into layer 7 “gravelly sands” (Table 1).

The inclusion grid spacing was adjusted according to the applied loads and the service settlement, ranging from 1.4 × 1.4 m to 2.9 × 2.9 m. The load transfer platform has a thickness of 0.5 m (Table 1). Through an iterative process with the structural engineering team, we converged on k_s values ranging from 1.5 to 4 MPa/m (Figure 5).

The CMC© solution is not intended to create piles designed to directly support the load of the structure individually, but rather to reduce the overall deformability of the soil through regularly spaced rigid elements. The concrete specified for the construction has a characteristic value of concrete compressive strength at 28 days $f_{ck} = 16$ MPa.

4.4 Settlement survey

The building was instrumented with surveying targets and monitored regularly for over a year during its construction.

The results presented here are remarkable for many reasons. Indeed, it remains paradoxically rare to have settlement monitoring of a structure, even though the very purpose of ground improvement works is precisely to ensure settlements remain within acceptable limits for the structure.

In general, the obstacles to this initiative can include the owner's refusal to allow instrumentation, difficulties in maintaining measurement targets on the structure throughout the multiple phases of construction, accidental destruction of

the surveying targets, and so on. Another non-technical potential obstacle is how the collected measurements may be used.

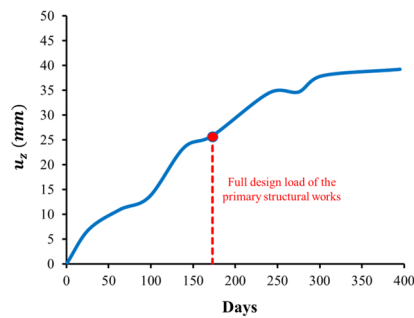


Figure 8. Settlement u_z monitoring at a building over 395 days. Each of the 10 points on the graph represents the average of five measurements taken at the four cardinal points and at the center of the building.

Indeed, the measurements must be capable of being interpreted and appropriately leveraged, even if they exceed the initially established thresholds, without necessarily resulting in a complete cessation of operations. For residential building structures, it should be noted that the achievable level of precision is generally in the order of centimeters.

The topographic targets were positioned at the surface of the raft foundation, at the four cardinal points and at the center, for a total of five measurement points. The measurements presented are the average values for a single monitored building, namely the one with the thickest compressible soils (26 m). Ten measurements were taken over 395 days of monitoring. The superstructure construction was completed after 175 days. Here, we have 220 days of monitoring following the completion of the main structural works (Figure 8). From a strictly technical standpoint, the loads associated with the finishing and fit-out works have not been considered.

4.5 Discussion and feedback

An exceptional thickness of 26 m of compressible soil was reinforced for this project.

The monitoring depicted in Figure 8 demonstrates that settlements commenced immediately from the onset of construction. Following the completion of construction, settlements continued to develop for an additional 125 days (up to day 300), after which they began a gradual deceleration, continuing until day 395. It is probable that, at the conclusion of this monitoring period, the settlement stabilization process had not yet been fully achieved. The total settlement was 39 mm, with differential settlements remaining within acceptable limits. It should be recalled that the target was 30 mm for total settlement.

The rapid onset of settlements is consistent with a predominantly silty and gravelly lithology, even though clayey layers have been observed. This rapid phenomenon also allowed for constructive discussion regarding the exceedance of the 30 mm limit. It should be noted that the settlement without soil improvement was 240 mm. To date, other measurements, such as radar interferometry, do not contradict the present measurements.

5 CONCLUSIONS

The presented project example offers practical insights for a raft foundation subjected to loads exceeding 100 kPa, with soil improvement extending to a depth of 26 m, and settlement values computed using moduli obtained through the ARSCOP methodology. In design, it is reasonable to account for the

weight of the excavated soil in order to determine a net surcharge on the ground, adopting a reload modulus close to the initial modulus. For heavily loaded raft foundations, the key issue lies in accurately determining the initial modulus, a task that the ARSCOP method facilitates. In the presented example, the modulus values were validated through settlement monitoring over an eight-month period following completion of the main structural works. In this case, the measures provide strong support for the ARSCOP approach.

6 ACKNOWLEDGEMENTS

We thank Gillian ERBEJA from Menard Lyon for collecting the data.

7 REFERENCES

- AFNOR 2021. NF EN ISO 22476-4 Reconnaissance et essais géotechniques - Essais en place - Partie 4 : Essai au pressiomètre Ménard. AFNOR.
- ARSCOP 2024. Journée de restitution des résultats du 26 septembre 2024, Paris, France.
- Arsonnet, G., Baud, J.P. and Gambin, M.P. 2005. Pressuremeter Tests Inside a Self-Bored Slotted Tube (STAF). In *ISP5 - Pressio 2005 - Symposium international - 50 ans de pressiomètre*. Vol. 1. Gambin, Magnan, Mesta, eds. Presse de l'ENPC/LCPC, 2005, 31-45.
- Baguelin, F., Jézéquel, J.-F. 1973. Le pressiomètre autoforeur. *Annales de l'ITBTP* 307-308, 133-160.
- Burlon, S., Frikha, W., Monaco, P. 2016. *Session report: Pressuremeter and Dilatometer*. 2016, Australian Geomechanics Society, Sydney, Australia.
- Briaud, J.L. (2013). The pressuremeter test: expanding its use. Ménard Lecture. *Proc. 18th International Conference on Soil Mechanics and Geotechnical Engineering*, Paris, France, 107-126.
- Brûlé, S. (2025). Ménard Pressuremeter Test and Dynamic Compaction. In: *ISP8 - Proc. 8th international symposium on pressuremeters*.
- Combarieu, O. 2006. Use of deformation moduli in geotechnical practice. *Rev. Fr. Geotech.* 114, 3-32.
- Gambin, M., Frank, R. 1982. *Ménard pressuremeter tests, Foundation Engineering*. Presses ENPC, Paris.
- Gambin, M. 1990. The history of pressuremeter practice in France. In: *ISP3 - Proc. 3rd international symposium on pressuremeters*. 5-24.
- Hoang, M.T., Cuira, F., Dias, D. et Miraillet, P. 2018. Estimation du rapport E/E_M : application aux radiers de grandes dimensions. In : *JNGG 2018 - Proc. 9^{ème} Journées Nationales de la Géotechnique et Géologie de l'Ingénieur*, Marne La Vallée, France.
- Hoang, M.T., Burlon, S. et Cuira, F. 2020. Prise en compte du niveau de déformation dans l'estimation des modules - Vers une approche unifiée pour le calcul des radiers et des semelles à partir du pressiomètre Ménard. Rapport de recherche du Projet National ARSCOP.
- Ménard, L. 1955. Pressiomètre, Paris, Brevet d'invention N°1.117.983 (1955).
- Ménard, L. 1957. Mesures in situ des propriétés physiques des sols. *Annales des Ponts et Chaussées* 3, 357-376.
- Ménard, L. 1962. Le pressiomètre Louis Ménard, Notice Générale D60: Règles d'utilisation des techniques pressiométriques et d'exploitation des résultats obtenus pour le calcul des fondations, France.
- Reiffsteck, P., Averlan, J.-L., Zerhouni M. (2018). *Essais de laboratoire pour la mécanique des sols et la géotechnique - Les outils pour la reconnaissance des sols et des roches*. Presses des Ponts.
- Winkler, E. 1867. Die Lehre von Elastizität und Festigkeit (on Elasticity and Fidity). Dominicus, 1198 Prague.